

Upgrade to Iterative Image Reconstruction (IR) in MDCT Imaging: A Clinical Study for Detailed Parameter Optimization Beyond Vendor Recommendations Using the Adaptive Statistical Iterative Reconstruction Environment (ASIR) Part2: The Chest

System-Upgrade auf iterative Bildrekonstruktion (IR) in der MDCT-Bildgebung: Eine klinische Studie zur detaillierten Parameteroptimierung jenseits der Herstellerempfehlungen am Beispiel der adaptiven statistischen iterativen Rekonstruktionsumgebung (ASIR): Teil 2: Der Thorax

Authors

F. G. Mueck, L. Michael, Z. Deak, M. K. Scherr, D. Maxien, L. L. Geyer, M. Reiser, S. Wirth

Affiliation

Institute for Clinical Radiology, Ludwig-Maximilians-University Hospital München, Munich

Key words

- thorax
- CT
- iterative image reconstruction
- statistical image noise
- dose reduction

eingereicht 27.6.2012
akzeptiert 14.2.2013

Bibliography

DOI <http://dx.doi.org/10.1055/s-0033-1335152>
Published online: 21.5.2013
Fortschr Röntgenstr 2013; 185: 644–654 © Georg Thieme Verlag KG Stuttgart · New York · ISSN 1438-9029

Correspondence

Fabian Gregor Mueck
Institut für klinische Radiologie,
Ludwig-Maximilians-University
München
Nussbaumstraße 20
80336 München
Germany
Tel.: ++49/895/1 60 92 01
Fax: ++49/895/1 60 92 02
fabian.mueck@med.uni-muenchen.de

Abstract



Purpose: To compare the image quality in dose-reduced 64-row CT of the chest at different levels of adaptive statistical iterative reconstruction (ASIR) to full-dose baseline examinations reconstructed solely with filtered back projection (FBP) in a realistic upgrade scenario.

Materials and Methods: A waiver of consent was granted by the institutional review board (IRB). The noise index (NI) relates to the standard deviation of Hounsfield units in a water phantom. Baseline exams of the chest (NI=29; LightSpeed VCT XT, GE Healthcare) were intra-individually compared to follow-up studies on a CT with ASIR after system upgrade (NI=45; Discovery HD750, GE Healthcare), n=46. Images were calculated in slice and volume mode with ASIR levels of 0–100% in the standard and lung kernel. Three radiologists independently compared the image quality to the corresponding full-dose baseline examinations (-2: diagnostically inferior, -1: inferior, 0: equal, +1: superior, +2: diagnostically superior). Statistical analysis used Wilcoxon's test, Mann-Whitney U test and the intraclass correlation coefficient (ICC). **Results:** The mean CTDIvol decreased by 53% from the FBP baseline to 8.0 ± 2.3 mGy for ASIR follow-ups; $p < 0.001$. The ICC was 0.70. Regarding the standard kernel, the image quality in dose-reduced studies was comparable to the baseline at ASIR 70% in volume mode (-0.07 ± 0.29 , $p = 0.29$). Concerning the lung kernel, every ASIR level outperformed the baseline image quality ($p < 0.001$), with ASIR 30% rated best (slice: 0.70 ± 0.6 , volume: 0.74 ± 0.61).

Conclusion: Vendors' recommendation of 50% ASIR is fair. In detail, the ASIR 70% in volume mode for the standard kernel and ASIR 30% for the lung kernel performed best, allowing for a dose reduction of approximately 50%.

Zusammenfassung



Ziel: Zielsetzung war im Rahmen eines System-Upgrade ein Vergleich der Bildqualität dosis-reduzierter 64-Zeilen CT's des Thorax, die mit unterschiedlichem Einfluss von Adaptiver Statistischer Iterativer Rekonstruktion (ASIR) rekonstruiert wurden, mit Voll-Dosis-Voruntersuchungen, welche mittels gefilterter Rückprojektion (FBP) rekonstruiert wurden.

Material und Methoden: Die Ethikkommission hatte keine Bedenken. Der Rauschindex (NI) bezieht sich auf die Standardabweichung in einem Wasserphantom. Baseline-Untersuchungen des Thorax (NI=29; LightSpeed VCT XT, GE) wurden nach System-Upgrade intra-individuell mit Follow-Up-Untersuchungen eines CT mit ASIR verglichen (NI=45; Discovery HD750, GE), n=46. Im Standard- und Lung-Kernel wurden Bilder mit 0–100% ASIR-Einfluss sowohl im Slice- als auch im Volumen-Modus berechnet. Drei Radiologen verglichen die Bildqualität mit der jeweiligen Voll-Dosis-Baseline (-2: diagnostisch schlechter, -1: schlechter, 0: gleich, +1: besser, +2: diagnostisch besser). Zur Analyse wurden der Wilcoxon, der Mann-Whitney-U-Test und die Intra-Class-Correlation's Koeffizient (ICC) verwendet.

Ergebnisse: Im Vergleich zur FBP-Baseline verringerte sich der durchschnittliche CTDIvol der ASIR-Follow-Ups um 53% auf $8,0 \pm 2,3$ mGy ($p < 0,001$, ICC=0,70). Mit Standard-Kernel war die durchschnittliche Bildqualität der dosis-reduzierten Studien mit denen der Baseline bei ASIR 70% im Volumen-Modus ($-0,07 \pm 0,29$, $p = 0,29$) vergleichbar. Für den Lung-Kernel war die Bildqualität jeder ASIR-Stufe besser als die der Baseline ($p < 0,001$), mit den besten Ergebnissen bei ASIR 30% (slice: $0,70 \pm 0,6$, volume: $0,74 \pm 0,61$).

Schlussfolgerung: Die Herstellerempfehlung von 50% ASIR ist in Ordnung. Im Detail waren aber mit dem Standard-Kernel und ASIR 70% im Volumen-Modus und mit dem Lung-Kernel und ASIR 30% die besten Ergebnisse zu erreichen und erlauben eine Dosisersparung von etwa 50%.

Introduction

Multidetector computed tomography (MDCT) is fast, readily available and provides high-resolution cross-sectional imaging which has an increasing impact on diagnostics and therapy. Therefore, the number of examinations is continuously rising [1]. Thus, computed tomography (CT) scanning leads to increasing radiation exposure which is widely discussed (1–3). Consequently, whether modalities such as ultrasound or magnetic resonance imaging (MRI) can be used alternatively has to be checked carefully. Sufficient image quality has to be achieved at the lowest possible dose level for the remaining large number of CT indications. With respect to this, several technical developments, such as automatic exposure control, automatic approaches to adapt the tube voltage to patient size and the planned examination type, and others, have already been successfully implemented in the past [1, 4–8].

Besides other developments, improved reconstruction algorithms aim to reduce image noise and are, therefore, a major focus of current developments in CT imaging [9–12]. This is promising for either improving image quality or reducing the dose. One particular example of algorithms in this field is the adaptive statistical iterative reconstruction technique (ASIR, GE Healthcare, Waukesha, WI), which is capable of two working modes: a) covering the xy-plane (slice mode), or b) additionally covering the z-axis (volume mode).

Although almost all vendors offer comparable options for their new scanner systems, only a limited number of publications have investigated ASIR effects in human chest imaging [13–20]. Current experiences using a 30%–50% ASIR are mainly based on phantom studies [19] and vendor recommendations [13, 16, 17, 21]. Many publications in this field are restricted to one or two ASIR blendings [13, 16, 17, 20]. Sub-analysis of the particularly promising volume mode is limited to a single case report [22]. Besides this, only one study did not restrict the evaluation to axial images but also included the diagnostically relevant multiplanar reformations [20]. However, neither of these studies in patients used the lung kernel for image reconstructions or the extended ASIR range, which can be varied between 0% and 100%. The aim of this clinical study (part 2) is on the one hand to compare image quality in dose-reduced 64-row CT of the chest at different levels of ASIR compared to full-dose baseline examinations reconstructed solely with filtered back projection (FBP) in a realistic upgrade scenario, and on the other hand to cross-check these results with those of a similar study concerning the abdomen (Part 1, [23]).

Materials and Methods:

The Declaration of Helsinki was strictly followed, and a waiver of consent was granted by the Institutional Review Board.

Phantom scans

A phantom (CATPHAN 500, Phantom Laboratory, Salem, NY) was scanned with the LightSpeed VCT XT (LS-VCT, General Electric, Waukesha, WI, USA) and also with the HD750 machine (GE) with and without the HD mode, using calculated, fixed parameters (200mA, 120kV), so that an identical radiation dose exposure was achieved compared to the follow-up patient study. Images in the standard kernel and lung kernel were compared visually.

The subjective analyses were based on the quantitative discrimination of line pairs in high contrast resolution and on the visibility and identifiability of round lesions as the low contrast resolution targets.

Patients, material and design

Consecutive patients with a baseline CT examination of the chest on the LS-VCT, and a CT follow-up within one year on the HD750 scanner were included, $n = 46$. The exclusion criteria included obvious changes with potential influence of the underlying disease on image quality, such as relevant alterations in tumor growth, lung infiltrations or systemic edema.

Relevant technical parameters of both CT scanners were identical, but LS-VCT used the V-Res detector (GE) whereas HD750 utilized the Gemstone detector (GE), which allows for an acquisition of 2496 projections per gantry rotation (HD scan mode = high-definition scan mode) instead of 984 projections compared to LS-VCT. As HD scan mode is a prerequisite for the volume mode of ASIR, it had to be used for follow ups, but it was not available for the baseline scans. According to the vendors' information, ASIR assumes that CT images contain the real information overlain by a dose-dependent level of noise. ASIR uses a noise-predicting model to separate this information and identifies and decreases the noise overlay iteratively. This process starts with FBP. The raw data is recalculated after each step of noise reduction in the prediction model resulting in an optimized raw dataset as the basis for the next step. This process is repeated until convergence of noise reduction and edge preservation effects are reached. ASIR offers two different modes to achieve these effects. In contrast to slice mode, the volume mode additionally takes adjacent information along 1.75 cm of the z-axis into account, and thus is more time-consuming but promises to be more effective. ASIR 2.0 can be merged with FBP for follow-ups in 10% steps of ASIR influence on the total reconstruction of the images (i.e., image reconstruction eventually uses an $x\%$ ASIR and $100\% - x\%$ FBP images).

Scanning protocols

Patients were in a supine, feet first position. Standardized contrast-enhanced chest scans were performed in the cranio-caudal direction. GE Healthcare uses a concept known as the noise index (NI). The noise index (NI) relates to the standard deviation of Hounsfield units in a water phantom of a specific size. A lookup table is used to map the patient-specific attenuation values measured on the CT projection radiograph ("scout" image) to tube current values for each gantry rotation according to a proprietary algorithm. The algorithm is designed to maintain the same image noise level as the attenuation values change from one rotation to the next. Within this study the NI [24, 25] was increased from 29 (baseline) to 45 for follow-up examinations, following the manufacturer's recommendation. Both scanners use the scout views to automatically modulate the mA per rotation in order to achieve the predefined NI level [16]. An overview of other relevant protocol parameters is shown in **Tab. 1**.

Processing and selection of images

AS the HD reconstruction kernel was not available for the baseline scanner and HD reconstructions are limited to a maximum scan field-of-view (sFOV) of 25 cm, HD reconstruction was not used in this study. Instead, the sFOV was identical for each HD750 study, and the display field-of-view (dFOV) was matched to the baseline study given. The raw data was reconstructed in both standard and lung kernels, resulting in nine settings for

each kernel: One setting with an ASIR of 0% (solely with FBP), and the remaining sets in both slice and volume mode, with ASIRs of 30%, 50%, 70%, and 100%, respectively. Therefore, a total of $n = 828$ series were available (46 CT scans * 2 kernels * 9 differing

image reconstructions). The duration of image reconstruction was measured manually. The resulting slices with a thickness of 0.625 mm were used to reformat image series matched to those used in the baseline examinations given:

► Standard kernel: axial, sagittal and coronal with a slice thickness of 3 mm

► Lung kernel: axial with a slice thickness of 2.5 mm

This reformation process was chosen because 0.625 mm slices were a prerequisite for ASIR reconstructions in the volume mode and for multiplanar reformations.

Three standard images were defined for each image series for the evaluation of body diameters and noise measurements (► Fig. 1):

a) Axial: at the level of the carina

b) Coronal: through the middle of the aortic valve

c) Sagittal: centric through the spine

Overall, these procedures ensured that the resulting HD750 datasets differed only with respect to ASIR level and mode, that the slices were identical with respect to position and size, and that the ASIR image series were as comparable as possible to the corresponding baseline series.

Reading of images and collection of data

A single workstation (Advantage workstation version 4.5, GE) with two identically calibrated displays was used for the data collection and the reading process. Viewing conditions were held constant according to the AAPM TG18 report [26] and checked daily for consistency.

The mean *image noise* was assessed as the unweighted mean value of standard deviations (SD) of Hounsfield Units using 100 [90 – 110] mm² circular regions of interest (ROIs). Measurements of soft tissue were taken at areas of muscle [1] and fat [2] that

Table 1 CT scan parameters of the baseline examination performed on a LightSpeed VCT XT and follow-up examination on a Discovery HD750 differing in noise index and number of projections per gantry rotation (HD scan mode = high-definition scan mode; usable on Discovery HD750).

Tab. 1 CT Scan-Parameter der Voruntersuchung (durchgeführt mit LightSpeed VCT XT) und der Nachuntersuchung (durchgeführt mit Discovery HD750). Diese unterschieden sich im Rauschindex (NI) und der Anzahl der Projektionen pro Röhrenrotation (HD-Scan Modus = high-definition Modus, nur verfügbar auf dem Discovery HD750).

	LightSpeed VCT XT (baseline)	Discovery HD 750 (follow-up)
noise index	29	45
detector	V-Res	Gemstone
high definition scanning	no (984 projections)	yes (2496 projection)
high definition image reconstruction	no	no
tube voltage (kv)	120	120
auto mA tube current range (mA)	80 – 600	80 – 600
rotation time (s)	0.5	0.5
collimation (mm)	0.625	0.625
detector length (mm)	40	40
beam pitch	0.984:1	0.984:1
table feed (mm)	39.37	39.37

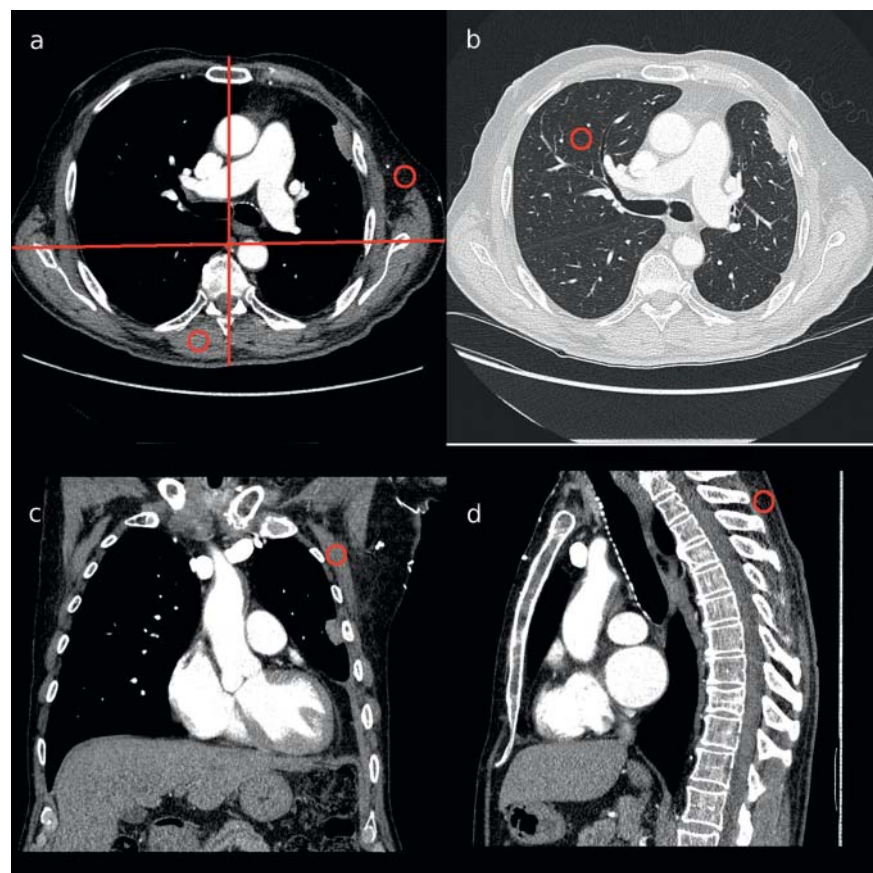


Fig. 1 Objective image evaluation: Lines indicate patient's diameters; circles show the region of interest used. For standard kernel: **a** Axial: through the carina, **c** Coronal: through the aortic valve, **d** Sagittal: centric through the spine. For lung kernel: **b** Axial: through the carina.

Abb. 1 Standardisierte Bilder für die quantitative (objektive) Auswertung: Die Linien zeigen die Patienten-Durchmesser, Kreise repräsentieren die verwendeten Region's of Interest (ROI). **a** Axial: durch die Carina **b** Coronal: durch die Aortenklappe **c** Sagittal: mittig durch die Wirbelsäule.

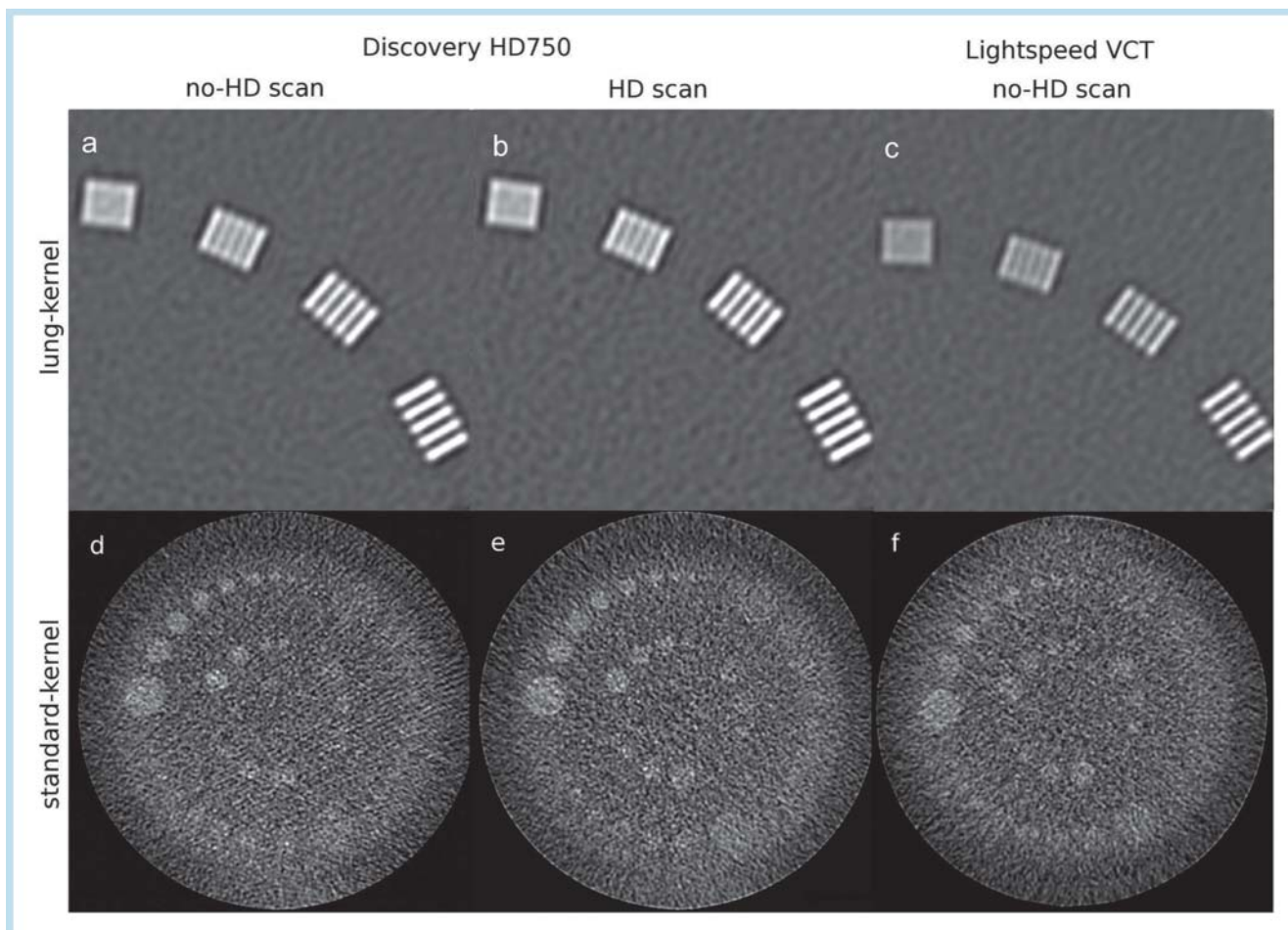


Fig. 2 A CATPHAN Phantom scanned with 2496 projections per rotation (HD scan) and with 984 projections per rotation (non-HD scan). **a, b, d,** and **e** were scanned on the Discovery HD750, while **c** and **f** were scanned on the LightSpeed VCT XT. Top: in lung kernel for high-contrast resolution (windowing: $W = 2000$, $L = 350$), and below: in standard kernel for low-contrast resolution (windowing: $W = 50$, $L = 50$). No differences are observable between non-HD and HD scans in high-contrast resolution. In contrast, low-contrast resolution of the HD750 scans was visually better compared to the LS-VCT data.

Abb. 2 Ein CATPHAN Phantom wurde, sowohl mit 2496 Projektionen pro Röhrenumlauf (HD Scans) als auch mit 984 Projektionen pro Röhrenumlauf (no-HD Scans) gescannt. **a, b, d** und **e** wurden auf dem Discovery HD750 gescannt, wohingegen **c** und **f** auf dem Lightspeed VCT XT gescannt wurden. Im oberen Bildanteil ist die hoch-Kontrast Auflösung im Lung-Kernel dargestellt (Fensterung: $W = 2000$, $L = 350$) und darunter für die niedrig-Kontrast-Auflösung im Standard-Kernel. (Fensterung: $W = 50$, $L = 50$). Für die hoch-Kontrast Auflösung war kein Unterschied zwischen HD und no-HD Scans erkennbar. Im Gegensatz dazu war das Ergebnis des Discovery HD750 für die niedrig-Kontrast Auflösung visuell besser im Vergleich zum Light-speed VCT XT.

were as homogenous as possible in standard kernel images. The lung kernel images were used to assess the noise in the lung tissue in the same way (► Fig. 1). Although the SD is a complex combination of normal texture and noise-generated inhomogeneities of the tissue samples, it still enables the estimation of the level of statistical noise as reasonably as possible. In addition, sagittal and coronal diameters of every patient were measured using a standardized procedure (► Fig. 1a).

Image quality was evaluated by three radiologists, blinded to the ASIR level and mode. The image quality for ASIR follow-up studies was compared to the corresponding baseline series using a five-point scale (+2: presumably diagnostically superior, +1: superior, 0: equal, -1: inferior, -2: presumably diagnostically inferior). In addition, the readers had to elucidate whether too much image noise, oversmoothing/blurring or another reason caused the diagnostically inferior image quality in the case of a rating of -2. A *total image quality* score was calculated as the mean value of ratings in the axial, sagittal and coronal planes. The lung kernel

evaluation criteria included the noise, contrast and sharpness of lung parenchyma, as well as the sharpness and contrast of central and peripheral lung vessels and airways. The criteria for the standard kernel included the noise, contrast and sharpness of the mediastinum, chest wall and muscle [27].

Statistical analysis

The Mann-Whitney U Test was used to compare ASIR images to the baseline, whereas the Wilcoxon rank-sum test was used to detect differences within the ASIR groups. The intraclass correlation coefficient (ICC) was calculated as a measure of inter-reader variability. All statistical testing was performed with SPSS 18.0.0 (PASW, Chicago, IL, USA).

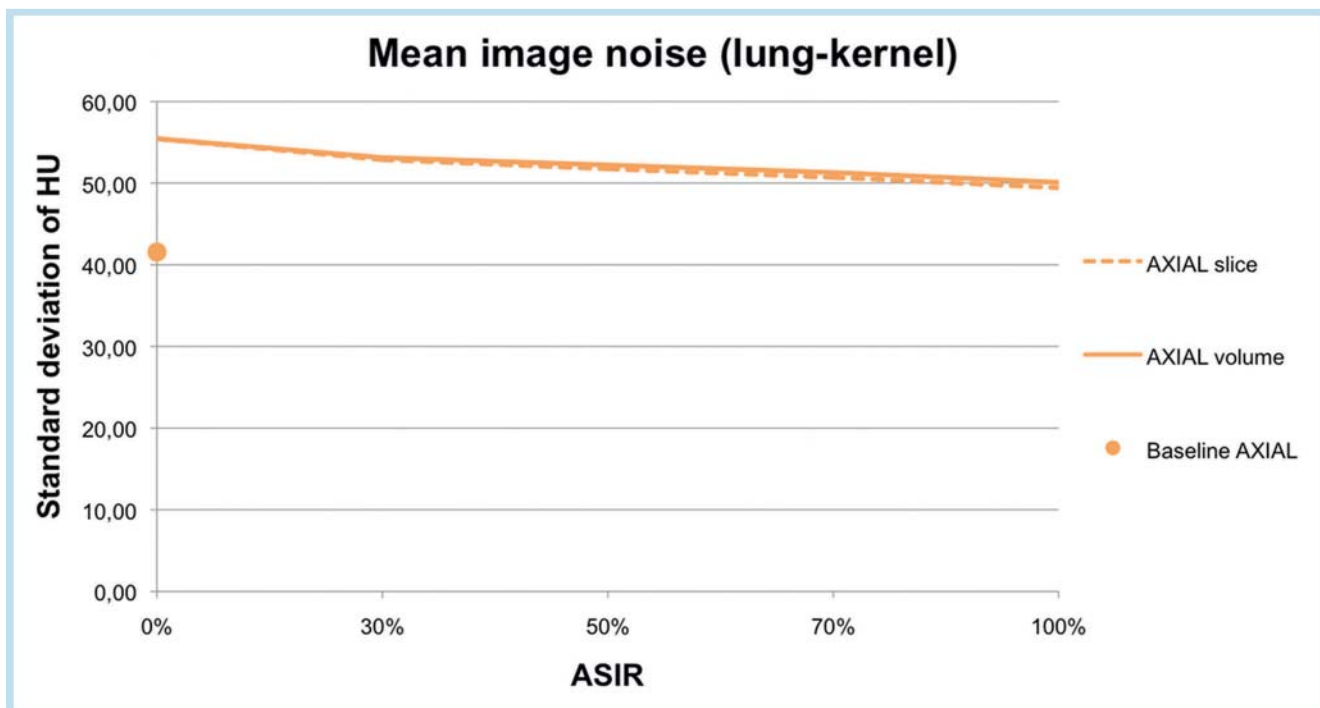


Fig. 3 Mean (SD) image noise in the lung kernel: Comparison of 50% dose-reduced ASIR to full-dose FBP baseline. Image noise of follow-ups was always higher compared to baseline (FBP) image noise, despite ASIR influence. There was only a significant difference compared to the baseline study at an ASIR of 0%, but not between slice and volume modes.

Abb. 3 Durchschnittliches (SD) Bildrauschen im Lung-Kernel: Vergleich von 50% dosis-reduzierten ASIR zu voll-dosis FBP-Baseline Untersuchungen. Das Bildrauschen der Folgeuntersuchungen war unabhängig vom ASIR Einfluß immer höher als das der Baseline (FBP). Jedoch war eine signifikante Differenz im Vergleich zur Baseline nur bei ASIR 0% festzustellen, aber nicht zwischen Slice- und Volumen-Modus.

Results

Phantom scans

No visual differences could be detected for the lung kernel (neither between the scanners nor between HD and non-HD scanning). Also no differences between HD and non-HD scans for the standard kernel were detected, but the HD750 image shows visually better contrast resolution compared to the LS-VCT scan (○ Fig. 2).

Patient scans

The resulting follow-up collective had the following parameters: age was 60 ± 15 [23–85] years, 26% female. The mean body weight was 83.1 ± 14.5 kg. The mean sagittal diameter at the level of the tracheal bifurcation was 24.84 ± 3.42 cm (baseline 24.64 ± 3.33 cm, $p=0.18$), and the mean coronal diameter was 37.95 ± 3.0 cm (baseline 37.94 ± 2.96 cm, $p=0.98$).

The *image reconstruction time* for the standard and lung kernel was 58 ± 9 seconds for both slice mode and FBP, increasing to 102 ± 15 seconds for the corresponding volume mode series.

The mean $CTDI_{vol}$ of the patient studies significantly decreased by 53% from 17.2 ± 6.9 (baseline) to 8.0 ± 2.3 mGy (ASIR follow-up; $p < 0.001$). The $CTDI_{vol}$ of the phantom scans was 7.9 ± 0.1 mGy.

Objective image noise

Increasing ASIR levels resulted in an approximately linear reduction of *image noise* in slice and volume mode for the standard and lung kernel.

Lung kernel

The mean image noise of follow-ups was always higher compared to the baseline, but only significant at an ASIR of 0%. Axial image reconstructions in the volume mode resulted in a slightly higher objective image noise than in the slice mode. However, this was not significant, neither between the two modes nor at the baseline examination ($p > 0.053$, ○ Fig. 3)

Standard kernel

Axial image reconstructions (ASIR 30%–100%) in the volume mode resulted in significantly higher image noise than in the slice mode ($p < 0.01$), whereas the values for MPRs were nearly identical (○ Fig. 4). When analyzing the image noise of axial pictures of the follow-ups, the ASIR levels of 30% and 50% in slice and volume mode and 70% in volume mode were able to provide image noise levels that were comparable ($p > 0.089$) to an ASIR 50% slice and an ASIR 70% volume and therefore almost identical to the full-dose baseline. ASIR levels below these limits cause higher image noise ($p=0.001$), whereas higher levels imply a noise reduction ($p \leq 0.018$). In contrast, the noise in MPR images was always higher compared to the full-dose baseline ($p \leq 0.002$), except for an ASIR of 100% (slice: $p=0.122$; volume: $p=0.235$).

Image quality Lung kernel

The *image quality* of the follow-ups outperformed the baseline examination at every ASIR level ($p < 0.001$), and performed best at an ASIR of 30% (slice: 0.70 ± 0.60 , volume: 0.74 ± 0.61). In particular, an ASIR of 30% was rated significantly better than an ASIR of 0% (i.e., solely calculated with FBP) in slice mode

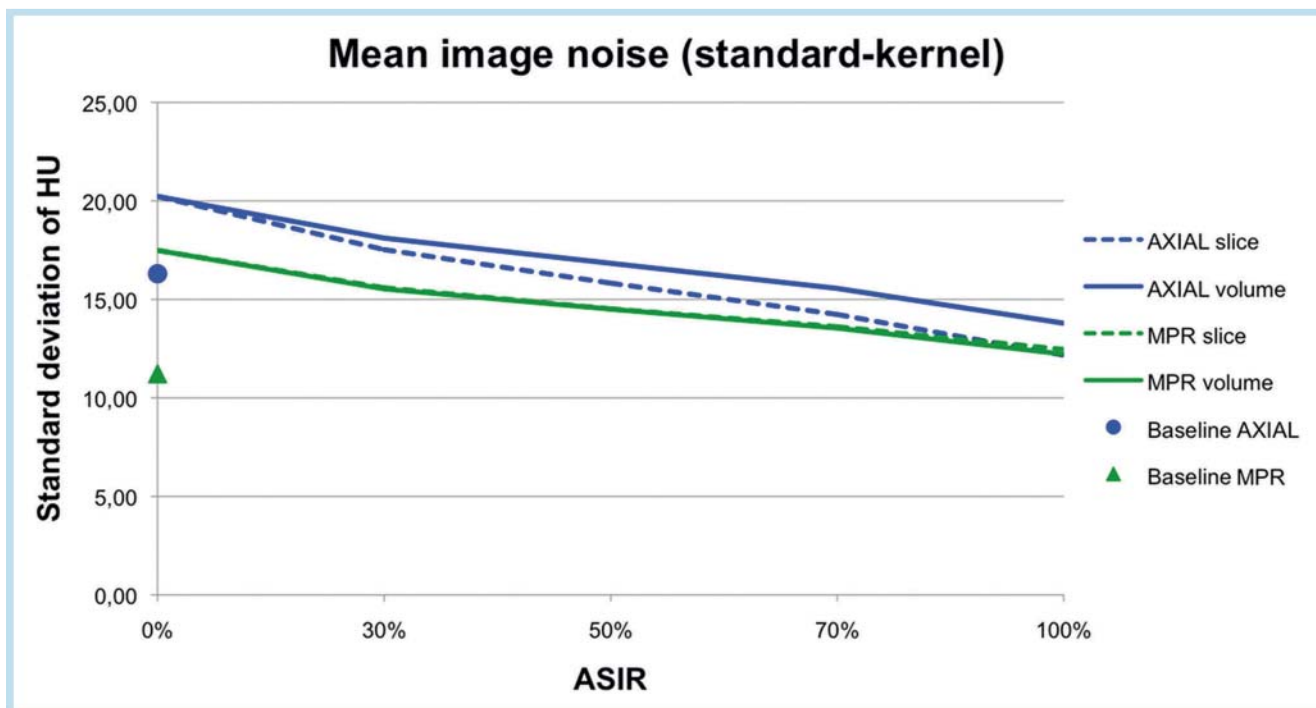


Fig. 4 Mean image noise in standard kernel: Comparison of 50% dose-reduced ASIR to full-dose FBP baseline. Increasing ASIR levels resulted in an approximately linear decrease. While follow-up image noise at an ASIR of 70% in the axial plane approached the baseline and undermatched with 100%, the MPRs' image noise is always higher than that of FBP reconstructed MPRs.

Abb. 4 Durchschnittliches Bildrauschen im Standard-Kernel: Vergleich von 50% dosis-reduzierten ASIR Studien zu voll-dosis Baseline Untersuchungen. Bei ansteigendem Einfluß von ASIR zeigte sich ein nahezu linear abnehmendes Bildrauschen. Die ASIR Folgestudien erreichten den Wert des Bildrauschens der Voruntersuchung bei ASIR 70% und lagen bei 100% ASIR Einfluß darunter. Das Bildrauschen der MPRs war immer höher als das Bildrauschen der mit FBP rekonstruierten MPRs.

($p=0.029$) and volume mode ($p=0.047$). A significant difference between slice mode and volume mode was limited to an ASIR of 100% ($p=0.002$) (Fig. 5, 6).

Standard kernel

The *total image quality* reached the level of the baseline examination with ASIR blendings of 70% (-0.07 ± 0.29 ; $p=0.289$) and 100% (-0.10 ± 0.42 ; $p=0.177$) solely in the volume mode. In contrast, all ASIR levels were rated significantly inferior to the baseline examination ($p<0.01$) for the slice mode. Even though the volume mode was almost always rated better than the slice mode, particularly with higher ASIR levels, this effect was only significant for 70% ($p=0.026$) and 100% ($p<0.001$). The results are summarized in Tab. 2, Fig. 6, 7.

Axial reformations in the slice mode performed significantly superior compared to MPRs with ASIRs of 0%-30% (0%: $p=0.004$; 30%: $p=0.021$), whereas ASIRs of 50%-70% performed comparably ($p \geq 0.347$) and an ASIR of 100% was inferior ($p<0.001$). In this manner, axial images in the volume mode only performed superior with an ASIR of 0% compared to MPRs ($p=0.004$).

Overall, the best particular results for MPRs were reached with an ASIR of 70% in the volume mode (-0.09 ± 0.34 ; $p=0.164$). The best ratings for axial images resulted from an ASIR of 70% blending in the volume mode (-0.10 ± 0.68 ; $p=0.90$). In contrast, an ASIR of 100% in the slice mode performed worst ($p<0.001$) and even ranged below the ASIR of 0% value (Tab. 2, Fig. 6, 7). Diagnostically inferior images (i.e., ratings with scores of -2) were limited to an ASIR of 0% and axial reconstructions with an ASIR of 100% in the slice mode. Within the ASIR 0% (i.e., FBP) sub-

group, these low ratings occurred in 9% of the images and were all caused by inadequate image noise. In contrast, for the subgroup of axial reconstructions with an ASIR of 100% in the slice mode, low rating scores occurred in 22% of the images and were all caused by oversmoothing.

Inter-reader variability

Acceptable inter-reader variability was observed for the lung kernel with an ICC of 0.67 (0.57–0.75; 95% confidence interval CI, $p<0.001$), and for the standard kernel, with an ICC of 0.70 (0.62–0.76; 95% CI, $p<0.001$).

Discussion:

As vendors especially advertise the dose-saving potential of their new systems and supply recommendations for new protocols, this study particularly aims to get the results of the typical situation when CT systems are upgraded. In this manner, the installation of a newly designed CT platform (such as the HD750) and its performance compared to its predecessor (such as the LS-VCT) were the inducement for closer inspection. In order to check whether the scanning protocols as supplied by the vendor are appropriate, we strictly followed the manufacturer's recommendations for CT scanning.

According to the highest ethical standards, every examination required a medical indication and the patient dose exposure had to be strongly minimized within the limits of the used system. We had to compare possible influences of HD scanning on the results,

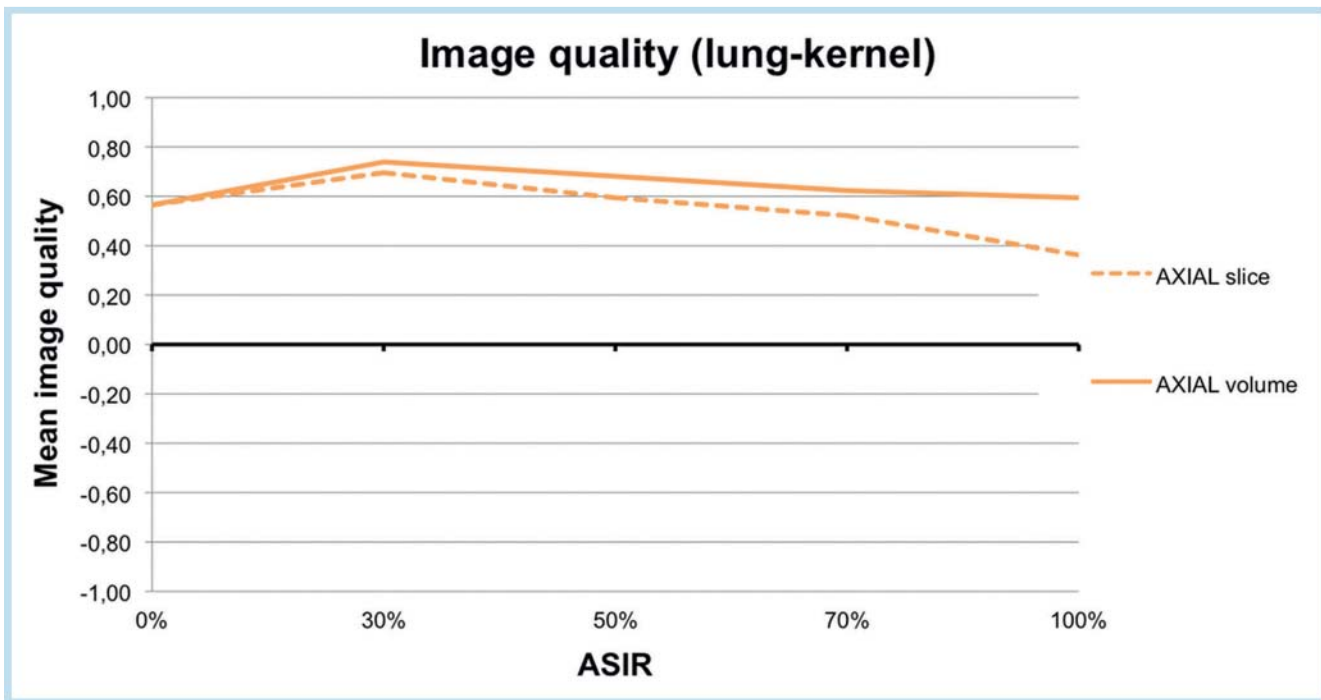


Fig. 5 Image quality in lung kernel: Comparison of 50 % dose-reduced ASIR to full-dose FBP baseline studies. Every level of the ASIR performed significantly superior to the baseline study. The best performance was evaluated at an ASIR of 30 %, whereas smoothing effects of high ASIR levels led to inferior performance, especially in the slice mode. Score: + 2 = presumably diagnostically superior, + 1 = superior, 0 = equal, - 1 = inferior, - 2 = presumably diagnostically inferior.

Abb. 5 Bildqualität im Lung-Kernel: Vergleich von 50 % dosis-reduzierten ASIR- zu voll-dosis FBP-Baseline Studien: Die mit ASIR berechneten Studien waren unabhängig vom ASIR Einfluß alle der Baseline Untersuchung überlegen. Am besten wurde die Bildqualität bei ASIR 30 % bewertet, wohingegen vor allem im Slice-Modus bei höherem ASIR Einfluss Weichzeichnungseffekte zu einer schlechteren Bewertung führten. Skala: + 2 = vermutlich diagnostisch besser, + 1 = besser, 0 = gleich, - 1 = schlechter, - 2 = vermutlich diagnostisch schlechter.

as data from HD scans was required as input for the volume mode and this option was not available on the baseline LS-VCT platform. It was not possible for ethical reasons to acquire HD and non-HD scans from the same patient during one examination. Instead, we compared these effects using a phantom.

Overall, the LS-VCT did not offer HD scanning but the protocols on the HD 750 were designed to match those protocols as closely as possible. Among others, this implicated the slice thicknesses used and also caused an unavoidable time interval between the two patient examinations. Comparability of the whole group is given, as the differences of the diameters of the patients' bodies are not significant, which are known to be the most important factors for modulation of the dose in CT scanning [28].

Three major changes between the two scanners contributed to the effects which were investigated in this study: V-Res/Gemstone detector, non-HD/HD scanning, and FBP/ASIR image calculation. A phantom was additionally scanned with both settings in order to estimate the particular contributions. HD scanning is known to be superior as long as images are additionally calculated with the HD kernel because the image matrix is able to display the benefits of higher resolution [17]. As long as no HD reconstruction is performed, no relevant differences between HD and non-HD scanning on the HD750 machine were observed. This implies no or only minor contribution of this parameter to image quality (• Fig. 2). In comparison, the low-contrast resolution of the LS-VCT scans was visually slightly inferior compared to the HD750 scans. In contrast to HD scanning, this implies a relevant contribution of the detector to the image quality, which is concordant with a recent study where the Gemstone detector

outperformed the V-Res detector regarding image noise by 7.9 – 20.6 %, depending on the slice thickness and reconstruction kernel [23, 29].

The mean image noise in the standard kernel decreased roughly linearly with increasing influence of ASIR (• Fig. 4). Similar results were observed in other publications [18, 19]. In this context, a higher noise reduction effect was observed solely for axial images in the slice mode. Since this mode does not take the z-axis into consideration, the observed effect could be attributed to a more effective but less realistic noise reduction (this is supported by the lower image quality especially of those images with high ASIR levels in • Fig. 7). As the dose of both groups is far above doses used in dedicated low-dose protocols for the lung, the dose difference between the baseline and the follow-up group can be expected to be negligible (of course this does not apply for soft tissue evaluation). Thus, the superior ratings compared to the FBP baseline with a higher dose (and thus lower image noise) might have to be credited to the new Gemstone detector in the HD750 machine. In addition, image noise is only one of obviously many factors which influence image quality. In detail, only the portion of “real statistical noise” is relevant and should be minimized. Other noise components, such as tissue inhomogeneities, show completely different influences and thus have to be preserved. The influence of edge enhancement for high-contrast images, such as the lung in the lung kernel, is much more relevant to the image quality than image noise. Once again, this does not apply to soft tissue evaluation. Nevertheless, the problem of noise measurements remains the same. The performed measurements are not able to distinguish between real statistical noise and the

Table 2 Mean subjective image quality ratings \pm standard deviation of dose-reduced images calculated with different Adaptive Statistical Iterative Reconstruction (ASIR) blending levels compared to full-dose filtered back projection (FBP) baseline examination (semi-quantitative 5-point scale: +2 = presumably diagnostically superior, +1 = superior, 0 = equal, -1 = inferior, -2 = presumably diagnostically inferior).

Tab. 2 Durchschnittlich subjektive Bewertungen der Bildqualität \pm Standardabweichung von Dosis-reduzierten Untersuchungen, die mit unterschiedlich starkem Einfluss des Adaptiven Statistischen Iterativen Rekonstruktions-Algorithmus (ASIR) berechnet wurden, im Vergleich zu einer Voruntersuchung mit voller Dosis, welche mittels gefilterter Rückprojektion (FBP) berechnet wurden (semi-quantitative 5 Punkte-Skala: +2 = vermutlich diagnostisch besser, +1 = besser, 0 = gleich, -1 = schlechter, -2 = vermutlich diagnostisch schlechter).

		ASIR level (%)				
	ASIR mode	0	30	50	70	100
Standard kernel						
Axial	Slice	-0.41 \pm 0.52 <i>p</i> < 0.001***	-0.17 \pm 0.38 <i>p</i> = 0.033*	-0.07 \pm 0.40 <i>p</i> = 0.357	-0.09 \pm 0.59 <i>p</i> = 0.418	-0.90 \pm 0.49 <i>p</i> < 0.001***
	Volume	-0.41 \pm 0.52 <i>p</i> < 0.001***	-0.16 \pm 0.58 <i>p</i> = 0.143	-0.03 \pm 0.38 <i>p</i> = 0.701	-0.01 \pm 0.68 <i>p</i> = 0.901	-0.10 \pm 0.60 <i>p</i> = 0.352
Sagittal/Coronal	Slice	-0.64 \pm 0.51 <i>p</i> < 0.001***	-0.32 \pm 0.41 <i>p</i> < 0.001***	-0.16 \pm 0.38 <i>p</i> = 0.020**	-0.17 \pm 0.40 <i>p</i> = 0.014*	-0.38 \pm 0.38 <i>p</i> < 0.001***
	Volume	-0.64 \pm 0.51 <i>p</i> < 0.001***	-0.30 \pm 0.47 <i>p</i> = 0.003**	-0.14 \pm 0.27 <i>p</i> = 0.012*	-0.09 \pm 0.34 <i>p</i> = 0.164	-0.09 \pm 0.49 <i>p</i> = 0.387
Total	Slice	-0.57 \pm 0.40 <i>p</i> < 0.001***	-0.27 \pm 0.30 <i>p</i> < 0.001***	-0.13 \pm 0.26 <i>p</i> = 0.006**	-0.14 \pm 0.36 <i>p</i> = 0.010*	-0.55 \pm 0.32 <i>p</i> < 0.001***
	Volume	-0.57 \pm 0.40 <i>p</i> < 0.001***	-0.25 \pm 0.38 <i>p</i> < 0.001***	-0.11 \pm 0.22 <i>p</i> = 0.020**	-0.07 \pm 0.29 <i>p</i> = 0.289	-0.10 \pm 0.42 <i>p</i> = 0.177
Lung kernel						
	ASIR mode	0	30	50	70	100
Axial	Slice	0.57 \pm 0.63 <i>p</i> < 0.001***	0.70 \pm 0.60 <i>p</i> < 0.001***	0.59 \pm 0.63 <i>p</i> < 0.001***	0.52 \pm 0.63 <i>p</i> < 0.001***	0.36 \pm 0.71 <i>p</i> = 0.003**
	Volume	0.57 \pm 0.65 <i>p</i> < 0.001***	0.74 \pm 0.61 <i>p</i> < 0.001***	0.68 \pm 0.61 <i>p</i> < 0.001***	0.62 \pm 0.60 <i>p</i> < 0.001***	0.59 \pm 0.67 <i>p</i> < 0.001***

Significance levels: (*) *p* < 0.05; (**) *p* < 0.01; (***) *p* < 0.001, *p* > 0.05 in bold.
Signifikanz-Level: (*) *p* < 0.05; (**) *p* < 0.01; (***) *p* < 0.001, *p* > 0.05 in Fettdruck.

“noise” caused by tissue inhomogeneities. As a consequence, the additional coverage of the z-axis in the volume mode may help the algorithm to differentiate between these two major noise components and may, therefore, focus the suppression of total noise more specifically on the real statistical component. Although it is not possible to prove this statement with the protocols used, it may be supported by identical findings within the abdominal part of the study. The higher noise of axial images compared to MPRs could be attributed to the primary voxel size with a higher resolution in the z-axis (0.625 mm axial slice thickness < FOV 50 cm/512 matrix = 0.975 mm), a somewhat sub-isotropic resolution [30].

The image quality in the lung kernel was rated best at an ASIR of 30% and is significantly superior compared to conventionally FBP-reconstructed image sets. This finding is also supported by other published recommendations of an ASIR of 30% in chest CT imaging, even though sharper kernels, such as the detail or bone kernel, were used instead of the lung kernel [13, 16–18, 20]. The image quality for soft tissue evaluation in the standard kernel was rated best at an ASIR of 70%. Even though this seems to be contrary to results in abdominal CT imaging which recommend the use of a 30%–50% ASIR, the findings of both studies are concordant considering that the abdominal studies were performed with a higher CDTI [19, 21] and that the more the dose is reduced, the more the particular ASIR effects seem to contribute to the appropriate enhancement of the image quality [18]. Furthermore, a recent study with a comparable design supports corresponding results for the CT examination of the abdomen and pelvis [14, 23].

An oversmoothing effect is known to appear when using very high ASIR levels, particularly in the slice mode, resulting in both low image noise and inferior image quality [13, 15, 17, 21]. Obviously, image quality is not only a consequence of image noise but also of edge preservation [13]. This effect of high-contrast kernels, such as the lung kernel, lead to a reduction of the image quality at ASIR levels of 50–100%, especially in the slice mode. A comparable effect for the standard kernel appeared for an ASIR of 100% in the volume mode, and for 70–100% in the slice mode.

Limitations of the study:

- ▼
- ▶ For ethical reasons, follow-up examinations had a medically indicated minimum time delay and, therefore, dose reduction was not a variable but a consequence of the protocols provided by the vendor.
- ▶ The study design allowed the influence of three different major variables. However, results indicate no/negligible influence of HD scanning (as long as it was performed without HD image reconstruction). The detector might be awarded 10–20% of the effects detected and led to a corresponding minor shifting of curves [29]. The remaining major part is contributed to the ASIR.
- ▶ Apart from changes in the patients' body weights, the underlying disease may also influence image quality. However, none of the patients had to be excluded for this reason.
- ▶ Although the rating criteria were according to guidelines on quality criteria for chest CT examinations, this does not allow final conclusions regarding diagnostic safety. Despite the at-

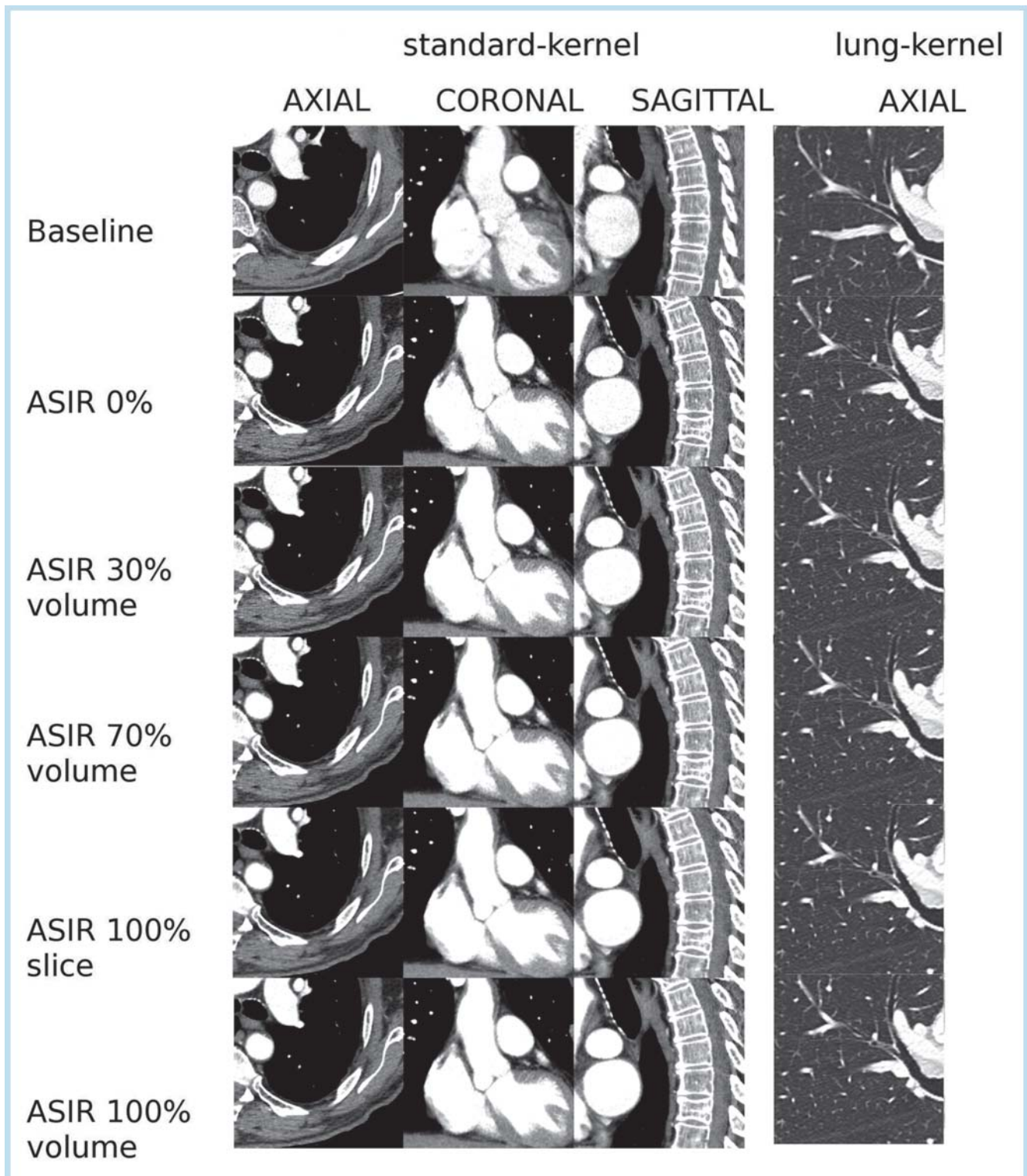


Fig. 6 Composed images from one patient in the standard kernel (all planes) and in the lung kernel (axial plane). Examples of the full-dose baseline as the reference study and ASIR calculated images at different ASIR levels of the dose-reduced follow-up study. Compared to the baseline, an ASIR of 0% showed up with more image noise according to the reduced dose. The noise decreases with increasing ASIR blendings, but can result in oversmoothing images, especially at ASIR 100% in slice mode.

Abb. 6 Bildbeispiele eines Patienten im Standard-Kernel (alle Ebenen) und im Lung-Kernel (axiale Ebene): Beispiele der voll-dosis Baseline-Untersuchung als Referenz und dosis-reduzierten ASIR-Bildern, die mit unterschiedlichem ASIR-Einfluß berechnet worden sind. Verglichen mit der Baseline zeigten sich ASIR 0% Bilder mit einer erhöhtem Bildrauschen was bei der reduzierten Dosis verständlich ist. Das Bildrauschen verringert sich mit zunehmendem Einfluß von ASIR auf die Bildberechnung, kann aber zu sehr weichgezeichneten Bildern führen, vorallem bei ASIR 100% im Slice-Modus.

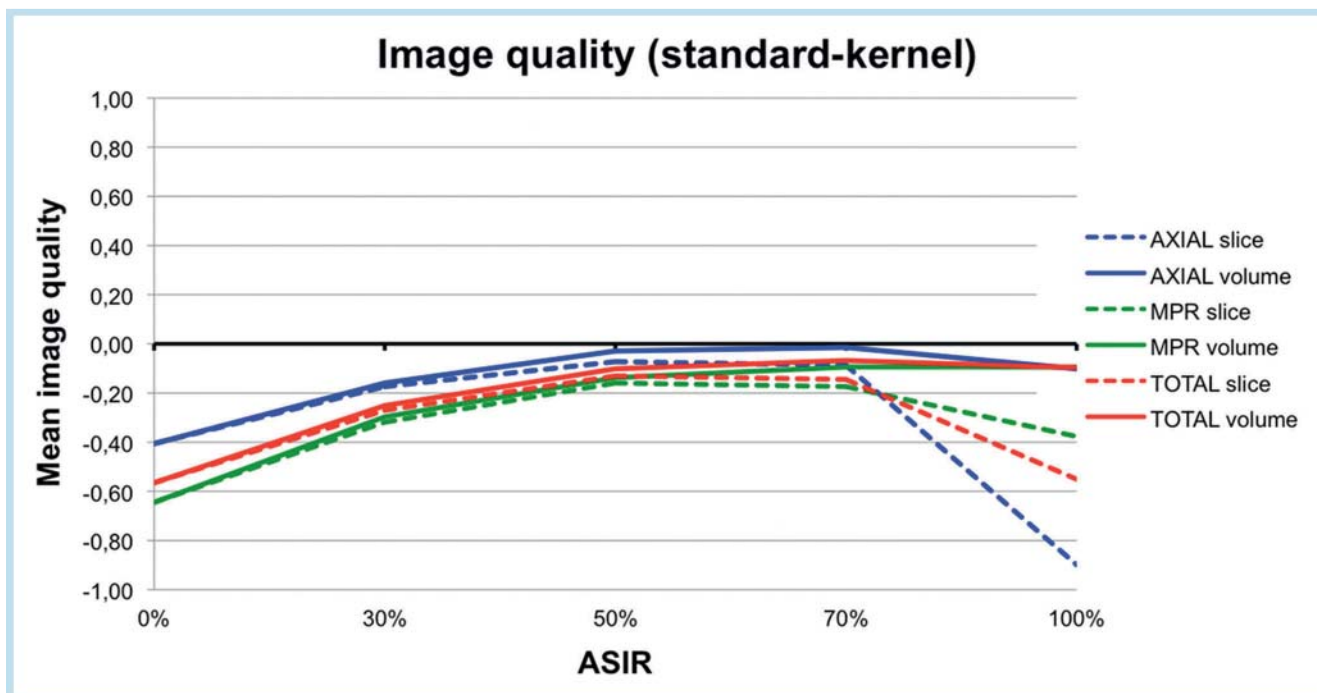


Fig. 7 Image quality in the standard kernel: Comparison of 50% dose-reduced ASIR to full-dose FBP baseline studies. With increasing levels of ASIR, the image quality of the follow-up study approached the value "0" as the reference image quality of the baseline and performed best at an ASIR of 70% in the volume mode. Axial images at an ASIR of 100% in slice mode performed even inferior to the ASIR of 0%, i. e., the FBP series at the same dose level. Score: + 2 = presumably diagnostically superior, + 1 = superior, 0 = equal, - 1 = inferior, - 2 = presumably diagnostically inferior.

Abb. 7 Bildqualität im Standard-Kernel: Vergleich von 50% dosis-reduzierten ASIR- zu voll-dosis FBP-berechneten Studien. Mit ansteigendem Einfluß von ASIR erreichte die Bildqualität der Folgeuntersuchungen den Wert „0“, definiert als Referenz durch die Baseline-Untersuchung, und stellte sich am besten bei einem ASIR-Einfluss von 70% im Volumen Modus dar. Die axialen Bilder bei ASIR 100% im Slice-Modus jedoch sogar schlechter als ASIR 0%, welches ausschließlich mit FBP berechnete Bildern bei identischer Dosis entspricht. Skala: + 2 = vermutlich diagnostisch besser, + 1 = besser, 0 = gleich, - 1 = schlechter, - 2 = vermutlich diagnostisch schlechter.

tempt to keep these effects as low as possible, ratings of image quality were restricted to a subjective image impression.

► Results are limited to a specific vendor, here GE Healthcare. Overall, the vendors' recommendations for upgrading to iterative image reconstruction were fair, but not ideal. With a 50% dose reduction, an ASIR of 30% even enhances image quality for the lung kernel in both modes, while for the standard kernel, an ASIR of 70% in the volume mode leads to an image quality that is similar to full-dose FBP images. Comparable to the setup of this study, most users follow the vendors' recommendations and thus the results of this study should also apply for their specific environment. For different baseline dose levels there might be a varying dose reduction potential. However, although different algorithms and study protocols were used, the reported dose reduction potential of ASIR ranged from 35% [31] to 64% [32]. When considering the particular upgrade scenario of our study, the iterative image reconstruction algorithm was the major factor for dose reduction in CT imaging of the chest, whereas a more sensitive detector might have contributed to additional minor dose savings as well. Although high-definition imaging (i. e., HD scanning and HD reconstruction) is proven to be superior [17], it showed no relevant impact in this study with a standard FOV and without HD data reconstruction. Iterative reconstruction algorithms significantly enhance image quality (XH HU), even for low-dose examinations, and a combination of low-dose protocols, HD imaging and iterative image reconstruction may be highly promising. However, this would require separate reconstructions of the left/right lungs in HD-FOVs of < 25 cm [17].

In the future, vendors will have to consider the implementation of upgraded computational power to keep this procedure fast enough for the daily routine, especially for the promising upcoming model-based approaches, which are even more complex, as they additionally consider exact geometrical features of the patient, the detectors and the beam distribution [33].

References

- Hall EJ, Brenner DJ. Cancer risks from diagnostic radiology. *Br J Radiol* 2008; 81 (965): 362–378
- Brenner DJ, Elliston CD. Estimated radiation risks potentially associated with full-body CT screening. *Radiology* 2004; 232: 735–738
- Galanski M, Nagel HD, Stamm G. CT-Expositionspraxis in der Bundesrepublik Deutschland. *Fortschr Röntgenstr* 173 (2001): R1–66
- Kubo T, Lin PJ, Stiller W et al. Radiation dose reduction in chest CT: a review. *Am J Roentgenol* 2008; 190: 335–43
- Dougeni E, Faulkner K, Panayiotakis G. A review of patient dose and optimisation methods in adult and paediatric CT scanning. *Eur J Radiol*. [Review]. 2012; 81: e665–683
- Ghoshhajra BB, Engel LC, Karolyi M et al. Cardiac Computed Tomography Angiography With Automatic Tube Potential Selection: Effects on Radiation Dose and Image Quality. *J Thorac Imaging* 2013; 28 (1): 40–48
- Gosch D, Stumpp P, Kahn T et al. Performance of an automatic dose control system for CT: anthropomorphic phantom studies. *Fortschr Röntgenstr* 183 (2011): 154–162
- Nagel HD, Stumpp P, Kahn T et al. Performance of an automatic dose control system for CT: specifications and basic phantom tests. *Fortschr Röntgenstr* 183 (2011): 60–67

- 9 Thibault JB, Sauer KD, Bouman CA et al. A three-dimensional statistical approach to improved image quality for multislice helical CT. *Med Phys* 2007; 34: 4526–4544
- 10 Fleischmann D, Boas FE. Computed tomography—old ideas and new technology. *Eur Radiol* 2011; 21: 510–517
- 11 Kropil P, Lanzman RS, Walther C et al. Dosisreduktion und Bildqualität in der MDCT des Oberbauchs: Potenzial eines adaptiven Nachverarbeitungsfilters. *Fortschr Röntgenstr* 2010; 182: 248–253
- 12 Kropil P, Cohnen M, Andersen K et al. Bildqualität in der Multidetektor-CT der Nasennebenhöhlen: Potenzial zur Dosisreduktion bei Anwendung eines adaptiven Nachverarbeitungsfilters. *Fortschr Röntgenstr* 2010; 182: 973–978
- 13 Leipsic J, Nguyen G, Brown J et al. A prospective evaluation of dose reduction and image quality in chest CT using adaptive statistical iterative reconstruction. *Am J Roentgenol* 2010; 195: 1095–1099
- 14 Qi LP, Li Y, Tang L et al. Evaluation of dose reduction and image quality in chest CT using adaptive statistical iterative reconstruction with the same group of patients. *Br J Radiol* 2012; 85 (1018): e906–e911
- 15 Yanagawa M, Honda O, Yoshida S et al. Adaptive statistical iterative reconstruction technique for pulmonary CT: image quality of the cadaveric lung on standard- and reduced-dose CT. 2010; 17: 1259–1266
- 16 Prakash P, Kalra MK, Digumarthy SR et al. Radiation dose reduction with chest computed tomography using adaptive statistical iterative reconstruction technique: initial experience. *J Comput Assist Tomogr* 2010; 34: 40–45
- 17 Prakash P, Kalra MK, Ackman JB et al. Diffuse lung disease: CT of the chest with adaptive statistical iterative reconstruction technique. *Radiology* 2010; 256: 261–269
- 18 Singh S, Kalra MK, Gilman MD et al. Adaptive statistical iterative reconstruction technique for radiation dose reduction in chest CT: a pilot study. *Radiology* 2011; 259: 565–573
- 19 Hara AK, Paden RG, Silva AC et al. Iterative reconstruction technique for reducing body radiation dose at CT: feasibility study. *Am J Roentgenol* 2009; 193: 764–771
- 20 Honda O, Yanagawa M, Inoue A et al. Image quality of multiplanar reconstruction of pulmonary CT scans using adaptive statistical iterative reconstruction. *Br J Radiol* 2011; 84: 335–341
- 21 Prakash P, Kalra MK, Kambadakone AK et al. Reducing abdominal CT radiation dose with adaptive statistical iterative reconstruction technique. *Invest Radiol* 2010; 45: 202–210
- 22 Heilbron BG, Leipsic J. Submillisievert coronary computed tomography angiography using adaptive statistical iterative reconstruction – a new reality. *Can J Cardiol* 2010; 26: 35–36
- 23 Mueck FG, Korner M, Scherr MK et al. Upgrade to iterative image reconstruction (IR) in abdominal MDCT imaging: a clinical study for detailed parameter optimization beyond vendor recommendations using the adaptive statistical iterative reconstruction environment (ASIR). *Fortschr Röntgenstr* 2012; 184: 229–238
- 24 Kalra MK, Maher MM, Blake MA et al. Multidetector CT scanning of abdomen and pelvis: a study for optimization of automatic tube current modulation technique in 120 subjects [abstract]. In: Radiological Society of North America Scientific Assembly and Annual Meeting Program Oak Brook, Ill: Radiological Society of North America; 2003, 294
- 25 McCollough CH, Bruesewitz MR, Kofler JM et al. CT dose reduction and dose management tools: overview of available options. *Radiographics* 2006; 26: 503–512
- 26 Samei E, Badano A, Chakraborty D et al. Assessment of display performance for medical imaging systems: executive summary of AAPM TG18 report. *Med Phys* 2005; 32: 1205–1225
- 27 EUR 16262. Quality criteria for computed tomography. Available at: <http://www.dr.dk/guidelines/ct/quality/download/eur16262.w51> Accessed March 25 ee.
- 28 Zarb F, Rainford L, McEntee MF. AP diameter shows the strongest correlation with CTDI and DLP in abdominal and chest CT. *Radiat Prot Dosimetry* 2010; 140: 266–273
- 29 Deak ZDP, Wirth S, Reiser MF et al. Comparing the effect of two different CT detectors of different generations on image noise (IN): a phantom study. Abstract accepted for RSNA meeting 2011
- 30 Tsukagoshi S, Ota T, Fujii M et al. Improvement of spatial resolution in the longitudinal direction for isotropic imaging in helical CT. *Phys Med Biol* 2007; 52: 791–801
- 31 Pontana F, Duhamel A, Pagniez J et al. Chest computed tomography using iterative reconstruction vs filtered back projection (Part 2): image quality of low-dose CT examinations in 80 patients. *Eur Radiol* 21 (2011): 636–643
- 32 Yamada Y, Jinzaki M, Hosokawa T et al. Dose reduction in chest CT: Comparison of the adaptive iterative dose reduction 3D, adaptive iterative dose reduction, and filtered back projection reconstruction techniques. *Eur J Radiol* 2012; 81 (12): 4185–4195
- 33 Katsura M, Matsuda I, Akahane M et al. Model-based iterative reconstruction technique for radiation dose reduction in chest CT: comparison with the adaptive statistical iterative reconstruction technique. *Eur Radiol* 2012; 22 (8): 1613–1623